ONLINE SUPPLEMENT

Valsartan Regulates Myocardial Autophagy And Mitochondrial Turnover In Experimental Hypertension

Xin Zhang, M.D.[1], Zi-Lun Li, M.D., Ph.D.[1,3], John A. Crane[1], Kyra L. Jordan[1], Aditya S. Pawar, M.D.[1], Stephen C. Textor, M.D.[1], Amir Lerman, M.D.[2], Lilach O. Lerman, M.D., Ph.D.[1,2]

[1]Division of Nephrology and Hypertension and [2]Division of Cardiovascular Diseases, Mayo Clinic, Rochester, MN, United States; [3]Division of Vascular Surgery, The First Affiliated Hospital, Sun Yat-sen University, Guangzhou, China

Correspondence:

Lilach O. Lerman, MD, PhD, Division of Nephrology and Hypertension, Mayo Clinic, 200 First Street SW, Rochester, MN 55905. lerman.lilach@mayo.edu

Phone: (507)-266-9376; Fax: (507)-266-9316

METHODS

1. Experimental protocol

This study was approved by the Institutional Animal Care and Use Committee. Four experimental groups of domestic female pigs (50-60 Kg, n=7 each) were studied over 10 weeks of observation. Pigs were randomized to untreated shams (Normal), RVH (n=7), and RVH treated with either Valsartan (RVH+Valsartan, n=7) or conventional triple therapy including Hydralazine, Reserpine, and Hydrochlorothiazide (RVH+TT, n=7). All pigs were fed the same amount of isocaloric diets of standard chow containing 0.15-0.65% sodium chloride (NaCl), and had free access to water.

Unilateral RAS was induced by placing a local irritant coil in the right main renal artery, leading to gradual obstruction of its lumen within the following days, as previously described.[1] A telemetry transducer (TA-D70, Data Sciences International, MN) was implanted in the left femoral artery in each animal[2, 3] to continuously monitor blood pressure during the observation. The day-night patterns of the blood pressure were also evaluated as previously described.[4] The degree of RAS was determined by renal angiography at 6 weeks, before initiation of antihypertensive regimens.

Medications were started and fed with food 6 weeks later for 4 additional weeks. Magnetic resonance imaging (MRI) and multi-detector computed-tomography (MDCT) studies were then performed to assess left ventricle (LV) myocardial oxygenation, remodeling, and function. Blood samples were collected at the time of imaging studies.

For each in vivo study animals were weighed, induced with Telazol and xylazine (5 mg/kg and 2 mg/kg, respectively, intramuscular injection) and intubated. For MDCT, animals were anesthetized during study by continuous intravenous infusion of Ketamine and ventilated with room air. During MRI, pigs were maintained anesthetized by ventilation of 2% isoflurane-contained oxygen.

Three days following the completion of in vivo studies, pigs were euthanized, by intravenous sodium pentobarbital (100mg/kg, Fatal Plus, Vortech Pharmaceuticals, Fort Washington, PA).[5] Hearts were removed, preserved, and prepared for ex-vivo tissue studies.

2. Antihypertensive treatment and dosage determination

Valsartan (Molecular Weight 435.5) was delivered at 320mg daily. The dosage of TT was initiated at Reserpine 0.1 mg/day, hydralazine 25 mg/day, and hydrochlorothiazide 12.5 mg/day, then titered based on the telemetry records to achieve comparable blood pressure control to the RVH+Valsartan groups.[6]

3. Cardiac hemodynamic, oxygenation, and function

Cardiac function and structure were assessed in vivo using 64-slice multi-detector computer tomography (MDCT, Somatom Definition-64, Siemens Medical Solution, Forchheim, Germany).[3, 7, 8] Two parallel 6-mm-thick mid-LV levels were selected for evaluation of myocardial perfusion and LV function. A bolus injection of nonionic, low

osmolar contrast medium (Isovue-370, 0.33 ml/Kg over 2 seconds) into the right atrium was followed by a 50-s flow study during respiratory suspension. Subsequently, the entire LV was scanned 20 times throughout the cardiac cycle to obtain parameters of cardiac function, including LV end diastolic volume, E/A ratio, stroke volume, and ejection fraction. LV muscle mass was acquired at the end-diastole by tracing the LV endocardial and epicardial borders, and LV mass/chamber volume (M/V) calculated to assess remodeling,[9, 10] LV myocardial perfusion was measured at both baseline and after adenosine infusion to assess microvascular function. The rate pressure product (RPP; systolic blood pressure x HR) served as an index of oxygen demand. After a 15-minutes interval, the same process was repeated during a 5-minute intravenous infusion of adenosine (400μg/kg/min).[3, 7, 11] The images were analyzed with the Analyze™ software package (Biomedical Imaging Resource, Mayo Clinic, Rochester, MN).[7]

To assess LV myocardial oxygenation, pigs were positioned in the MRI scanner (Signa EXCITE 3T system, GE, Waukeshau, WI) and blood oxygen level dependent (BOLD) images (4-5 axial-oblique) were acquired along the cardiac short axis during suspended respiration.[7, 12] Gated Fast Gradient Echo sequence was used with TR/TE/number of echoes/Matrix size/FOV/Slice thickness/Flip angle=6.8 ms/1.6-4.8 ms/8/128x128/35/0.5 cm/30°. Data was acquired before and after intravenous injection of adenosine (400 mg/kg/min) through the ear vein catheter, to evaluate the oxygenation level under basal conditions and its response to a vasodilator. In each slice on T2*-weighted images obtained, the BOLD index, R2*, was estimated in each voxel by fitting the MR signal intensity vs. echo times to a single exponential function and calculating the MR intensity decay rate. Images were subsequently analyzed using MATLAB 7.10 (MathWorks, Natick, MA).

Blood samples were collected from inferior vena cava during in-vivo studies to measure plasma creatinine and aldosterone.

4. Ex vivo studies

1) Myocyte hypertrophy:

Wheat germ agglutinin (WGA, Invitrogen) staining was performed on tissue sections of left ventricular myocardium to assess cardiomyocyte hypertrophy. Immunoflurosecent images were taken at 40x magnification at areas of transversely cut muscle fibers and examined using a computer-aided image-analysis program (AxioVision® v4.7.2.0, and ZEN 2012, Carl Zeiss MicroImaging, Thornwood, NY). Cardiomyoctes with round nuclei were included for measurement. Lines were drawn to delineate the border of each cell according to WGA staining that highlights the cell membrane, then the area within the border were automatically calculated. Around 50-100 cardiomyocytes were measured and averaged for each animal.

2) Microcirculation:

The left-anterior-descending coronary artery was perfused with a radio-opaque polymer under physiological pressure, and a transmural portion of the LV was then prepared and scanned at 0.5° angular increments at 20-μm resolution, as previously

described.[2, 11, 13] The spatial density of microvessels (defined as diameters <500 μm) in the subepicardium and subendocardium was calculated and classified according to diameter as small (20-200 μm) and large (200-500 μm) microvessels. Expression of vascular endothelial growth factor (VEGF), angiopoietin-1 and hypoxia-inducible factor (HIF)-1α were examined by western blotting and immunofluorescence for angiogenesis.

3) Myocardial autophagy and mitochondrial turnover

Autophagy was examined by the expression of the autophagy initiator Beclin, autophagosome formation hallmarks autophagy-related gene (Atg)12-Atg5, and microtubule-associated protein1 light chain (LC) 3-II, as well as the LC3-II/LC3-I ratio. Expression of mammalian target of rapamycin (mTOR) was also assessed.
Apoptosis was evaluated by Terminal deoxynucleotidyl transferase dUTP nick end labeling (TUNEL) and caspase-3 staining, western blotting for Bax and Bcl-xL, and their ratio (Bax/Bcl-xL).
Mitochondrial degradation: Myocardial expression of dynamin-related protein (DRP) which participates selective degradation of mitochondria[14] was examined by Western blotting. Cardiomyocyte mitophagy was also examined by immunofluorescence staining for Parkin (green, Santa Cruz) and the mitochondrial outer membrane marker Tom20 (red, Santa Cruz) for Parkin translocation (yellow).[15, 16] Images were taken at 40x with a zoom factor of 1.5 using the LSM780 microscope (Carl Zeiss MicroImaging), and with a zoom factor of 2.5 for inserts. Parkin-translocation+ cells were counted to represent mitophagic cardiomyocytes.
Mitochondrial biogenesis Signals for mitochondrial biogenesis were detected by the expression of chief modulator peroxisome proliferator-activated receptor gamma coactivator (PGC)-1α,[17] and its effectors nuclear respiratory factor **(**NRF)-1, and uncoupling protein (UCP)-2. Mitochondrial respiratory chain subunits proteins were examined by cytochrome c oxidase (COX) I, COXIV and mitochondrial NADH dehydrogenase (MTND)-1.

4) Oxidative stress and fibrosis

Oxidative stress was assessed by dihydroethidium (DHE) staining and western blotting for the expression of NAD(P)H oxidase gp91. Myocardial fibrosis was evaluated by Masson's trichrome staining, and expression of tissue growth factor (TGF)-β and matrix metalloproteinase (MMP)-2.

5) Western blotting

Standard blotting protocols were followed, using specific polyclonal antibodies against target proteins VEGF (Santa Cruz 1:200), angiopoietin-1(Santa Cruz, 1:200), and HIF-1α(abcam, 1:1000) for angiogenesis; Beclin (abcam, 1:500), Atg12-Atg5 (Cell Signaling, 1:1000), LC3 (abcam, 1:500), and mTOR (abcam, 1:2000) for autophagy; Bax and Bcl-xL (both Santa Cruz, 1:200) for apoptosis; DRP-1 (Cell Signaling, 1:1000) for mitophagy; PGC-1α, NRF-1, and UCP-2 for mitochondrial biogenesis signals (all Abcam, 1:1000); MTCO1 (abcam, 1:2000), COXIV (Cell Signaling, 1:1000), and MTND-1 (abcam, 1:1000) for mitochondria production; NAD(P)H oxidase gp91 (abcam, 1:1000) for oxidative stress, and TGF-β and MMP-2 (both Santa Cruz, 1:200) for fibrosis.

Horseradish peroxidase secondary antibodies (GE Healthcare UK Limited) were used and chemiluminescence determined using the SuperSignal West Pico Chemiluminescent Substrate or SuperSignal West Femto Maximum Sensitivity Substrate (Thermo Scientific, IL) according to vendor's instructions. Glyceraldehyde 3-phosphate dehydrogenase (GAPDH, 1:5000 Covance, Emeryville, CA) served as loading control.

5. Statistics

Data are expressed as mean±SEM. Comparisons within groups were performed using the paired Student's *t*-test and among groups ANOVA followed by unpaired *t*-test. Statistical significance was accepted at $P < 0.05$.

REFRENCES FOR ONLINE SUPPLEMENT

1. Chade AR, Rodriguez-Porcel M, Grande JP, Krier JD, Lerman A, Romero JC, Napoli C, Lerman LO. Distinct renal injury in early atherosclerosis and renovascular disease. *Circulation*. 2002;106:1165-1171.
2. Zhu XY, Rodriguez-Porcel M, Bentley MD, Chade AR, Sica V, Napoli C, Caplice N, Ritman EL, Lerman A, Lerman LO. Antioxidant intervention attenuates myocardial neovascularization in hypercholesterolemia. *Circulation*. 2004;109:2109-2115.
3. Zhu XY, Daghini E, Chade AR, Napoli C, Ritman EL, Lerman A, Lerman LO. Simvastatin prevents coronary microvascular remodeling in renovascular hypertensive pigs. *J Am Soc Nephrol*. 2007;18:1209-1217.
4. Urbieta-Caceres VH, Zhu XY, Jordan KL, Tang H, Textor K, Lerman A, Lerman LO. Selective improvement in renal function preserved remote myocardial microvascular integrity and architecture in experimental renovascular disease. *Atherosclerosis*. 2012;221:350-358.
5. Juillard L, Lerman LO, Kruger DG, Haas JA, Rucker BC, Polzin JA, Riederer SJ, Romero JC. Blood oxygen level-dependent measurement of acute intra-renal ischemia. *Kidney Int*. 2004;65:944-950.
6. Zhang X, Eirin A, Li Z-L, Crane JA, Krier JD, Ebrahimi B, Pawar AS, Zhu X-Y, Tang H, Jordan KL, Lerman A, Textor SC, Lerman LO. Angiotensin receptor blockade has protective effects on the poststenotic porcine kidney. *Kidney Int*. 2013;84:767-775.
7. Li ZL, Woollard JR, Ebrahimi B, Crane JA, Jordan KL, Lerman A, Wang SM, Lerman LO. Transition from obesity to metabolic syndrome is associated with altered myocardial autophagy and apoptosis. *Arterioscler Thromb Vasc Biol*. 2012;32:1132-1141.
8. Rodriguez-Porcel M, Herrman J, Chade AR, Krier JD, Breen JF, Lerman A, Lerman LO. Long-term antioxidant intervention improves myocardial microvascular function in experimental hypertension. *Hypertension*. 2004;43:493-498.
9. Rosen BD, Edvardsen T, Lai S, Castillo E, Pan L, Jerosch-Herold M, Sinha S, Kronmal R, Arnett D, Crouse JR, 3rd, Heckbert SR, Bluemke DA, Lima JA. Left ventricular concentric remodeling is associated with decreased global and regional systolic function: The multi-ethnic study of atherosclerosis. *Circulation*. 2005;112:984-991.
10. Lorell BH, Carabello BA. Left ventricular hypertrophy: Pathogenesis, detection, and prognosis. *Circulation*. 2000;102:470-479.
11. Urbieta Caceres VH, Lin J, Zhu XY, Favreau FD, Gibson ME, Crane JA, Lerman A, Lerman LO. Early experimental hypertension preserves the myocardial microvasculature but aggravates cardiac injury distal to chronic coronary artery obstruction. *Am J Physiol Heart Circ Physiol*. 2011;300:H693-701.
12. Warner L, Glockner JF, Woollard J, Textor SC, Romero JC, Lerman LO. Determinations of renal cortical and medullary oxygenation using blood oxygen level-dependent magnetic resonance imaging and selective diuretics. *Invest Radiol*. 2011;46:41-47.

13. Rodriguez-Porcel M, Lerman A, Ritman EL, Wilson SH, Best PJ, Lerman LO. Altered myocardial microvascular 3d architecture in experimental hypercholesterolemia. *Circulation*. 2000;102:2028-2030.
14. Marsboom G, Toth PT, Ryan JJ, Hong Z, Wu X, Fang YH, Thenappan T, Piao L, Zhang HJ, Pogoriler J, Chen Y, Morrow E, Weir EK, Rehman J, Archer SL. Dynamin-related protein 1-mediated mitochondrial mitotic fission permits hyperproliferation of vascular smooth muscle cells and offers a novel therapeutic target in pulmonary hypertension. *Circ Res*. 2012;110:1484-1497.
15. Arena G, Gelmetti V, Torosantucci L, Vignone D, Lamorte G, De Rosa P, Cilia E, Jonas EA, Valente EM. Pink1 protects against cell death induced by mitochondrial depolarization, by phosphorylating bcl-xl and impairing its pro-apoptotic cleavage. *Cell Death Differ*. 2013;20:920-930.
16. Vives-Bauza C, Zhou C, Huang Y, Cui M, de Vries RL, Kim J, May J, Tocilescu MA, Liu W, Ko HS, Magrane J, Moore DJ, Dawson VL, Grailhe R, Dawson TM, Li C, Tieu K, Przedborski S. Pink1-dependent recruitment of parkin to mitochondria in mitophagy. *Proc Natl Acad Sci U S A*. 2010;107:378-383.
17. Canto C, Auwerx J. Pgc-1alpha, sirt1 and ampk, an energy sensing network that controls energy expenditure. *Curr Opin Lipidol*. 2009;20:98-105.

Figure S1

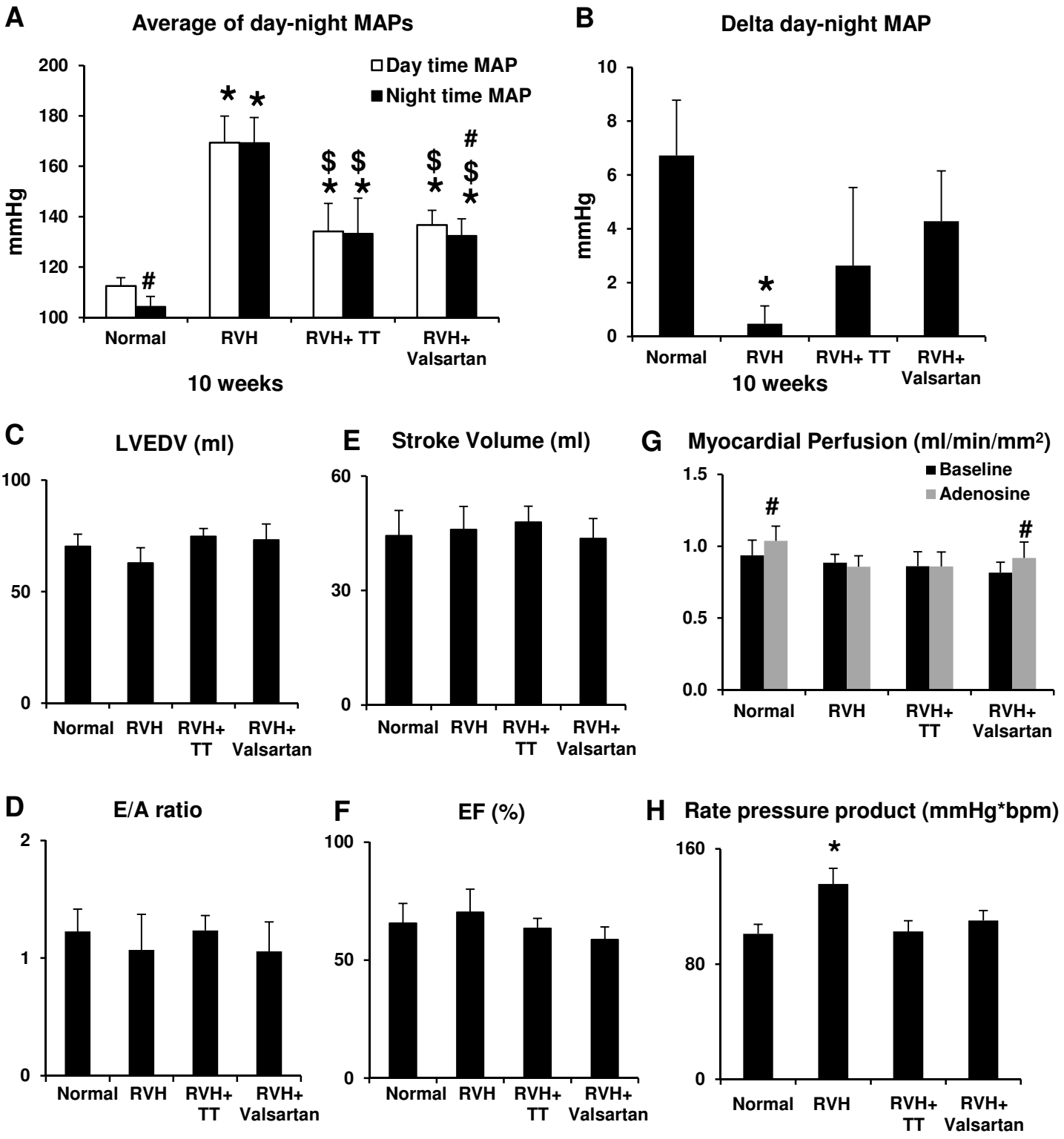

Figure S1. A and B: Diurnal patterns of mean arterial pressure in Normal, renovascular hypertension (RVH), RVH+triple therapy (TT) and RVH+Valsartan pigs. C-F: Diastolic and systolic function was relatively preserved in early RVH. G: Myocardial perfusion measured by multi-detector CT showed diminished response to adenosine in RVH that was normalized only by Valsartan. H: Rate-pressure product indicated elevated oxygen demand in RVH but restored by both regimens. *$p<0.05$ vs. Normal; $^{\$}p<0.05$ vs. RVH; $^{\#}p<0.05$ vs. its control.

Figure s2

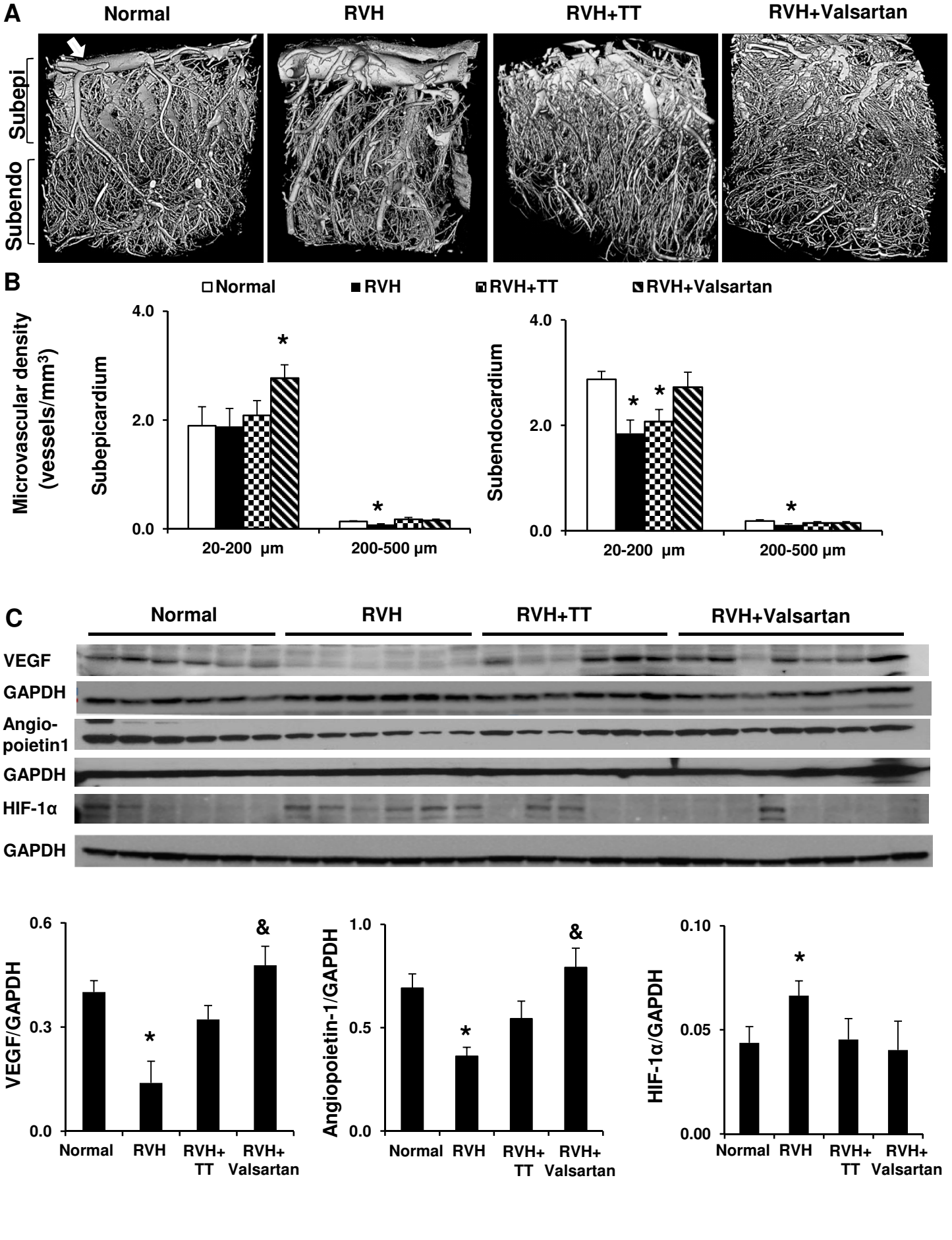
A
Normal
RVH
RVH+TT
RVH+Valsartan
Subepi
Subendo
B
Normal
RVH
RVH+TT
RVH+Valsartan
Microvascular density (vessels/mm3)
Subepicardium
Subendocardium
4.0
2.0
0.0
20-200 μm
200-500 μm
C
Normal
RVH
RVH+TT
RVH+Valsartan
VEGF
GAPDH
Angio-poietin1
GAPDH
HIF-1α
GAPDH
VEGF/GAPDH
Angiopoietin-1/GAPDH
HIF-1α/GAPDH
0.6
0.3
0.0
1.0
0.5
0.10
0.05
0.00
Normal
RVH
RVH+ TT
RVH+ Valsartan

Figure s2 (Continued)

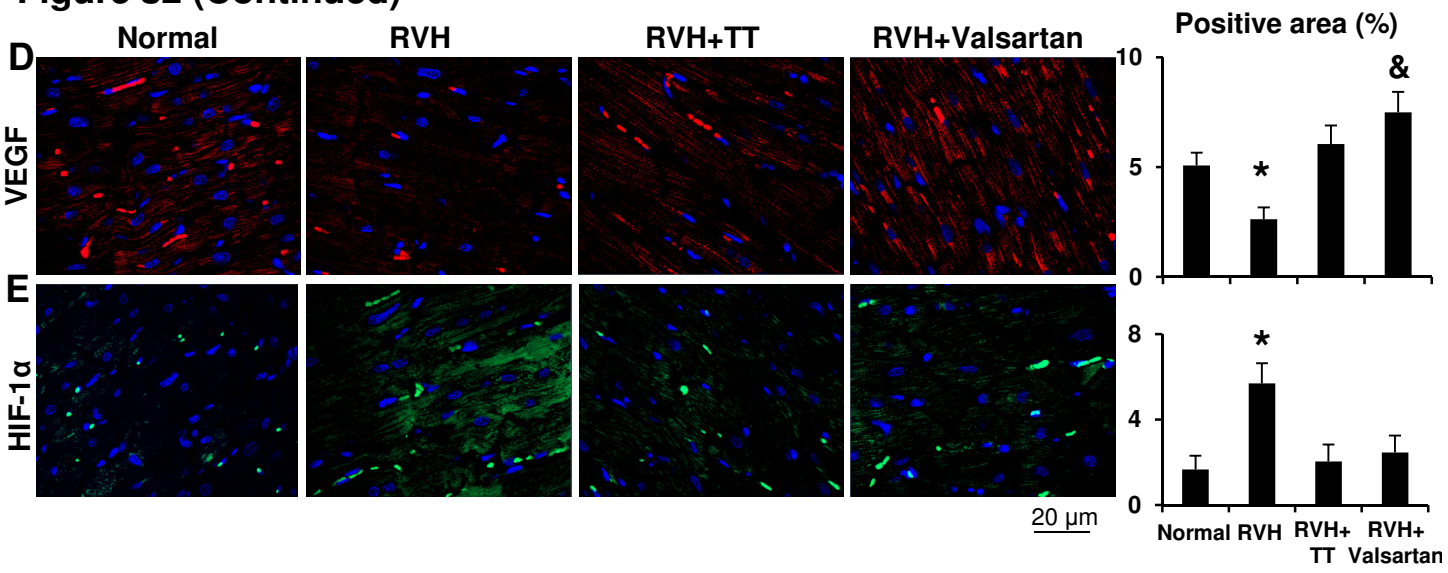

Figure S2. A: Representative 3-D micro CT images of the LV myocardium in the 4 groups. White arrow indicates the left anterior descending artery. B: Quantification of microvascular density. C: Expression of the angiogenic factors vascular endothelial growth factors (VEGF), angiopoietin-1 and hypoxia-inducible factor (HIF)-1α. D and E: Representative immunofluorescence images (40x) and quantification for VEGF (red) and HIF-1 α (green) expression in the myocardium. Valsartan restored microvascular density, and upregulated angiogenesis to a greater extent than TT. *$p<0.05$ vs. Normal; $^{\&}p<0.05$ vs. RVH+TT.

Figure s3

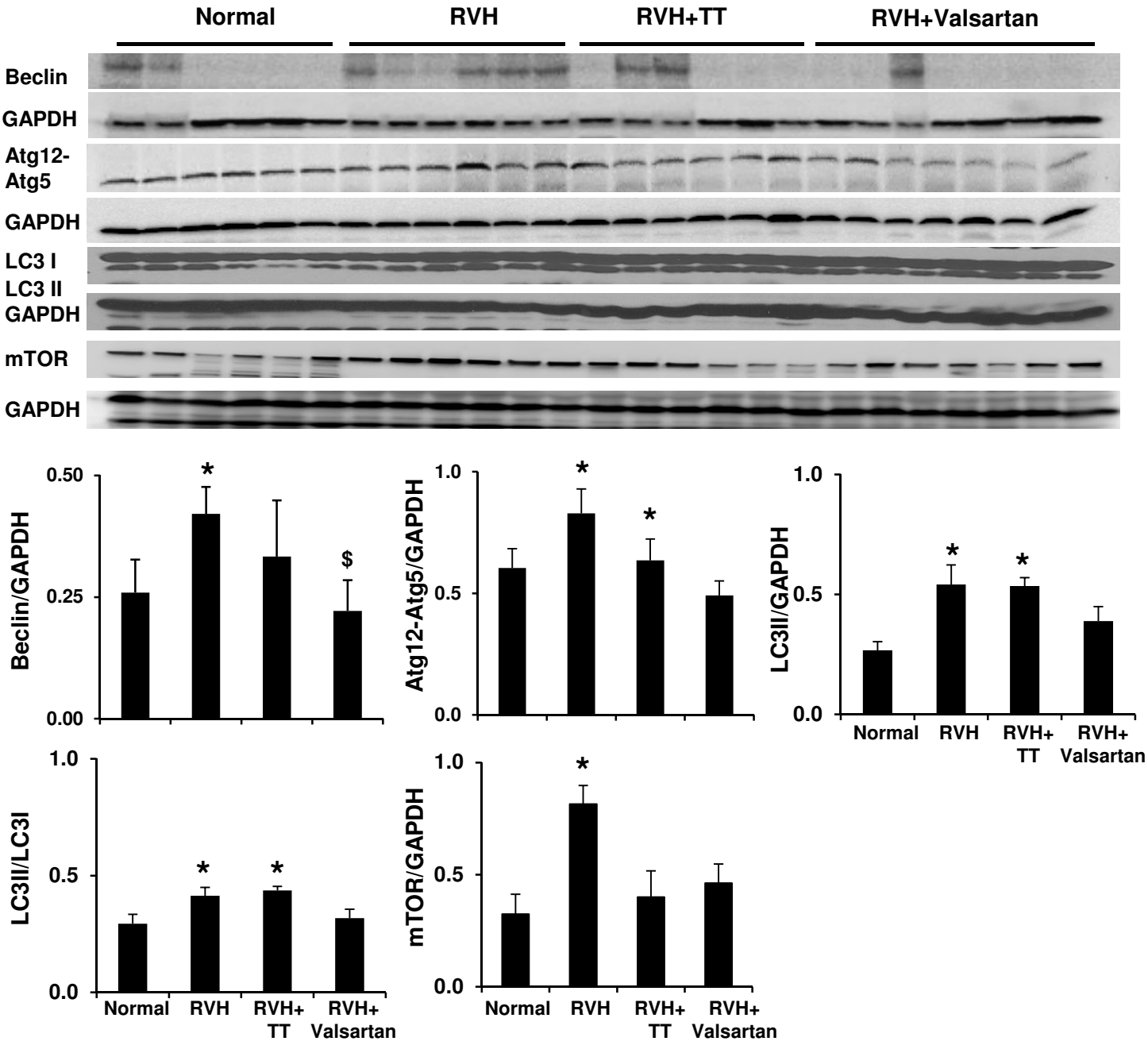

Figure S3. Expression of autophagic proteins in Normal, RVH, RVH+TT and RVH+Valsartan pig hearts. Atg: autophagy-related gene; LC3: microtubule-associated protein1 light-chain-3; mTOR: mammalian target of rapamycin. Valsartan alone reversed enhanced autophagy in RVH myocardium. *$p<0.05$ vs. Normal; $^{\$}p<0.05$ vs. RVH.

Figure s4

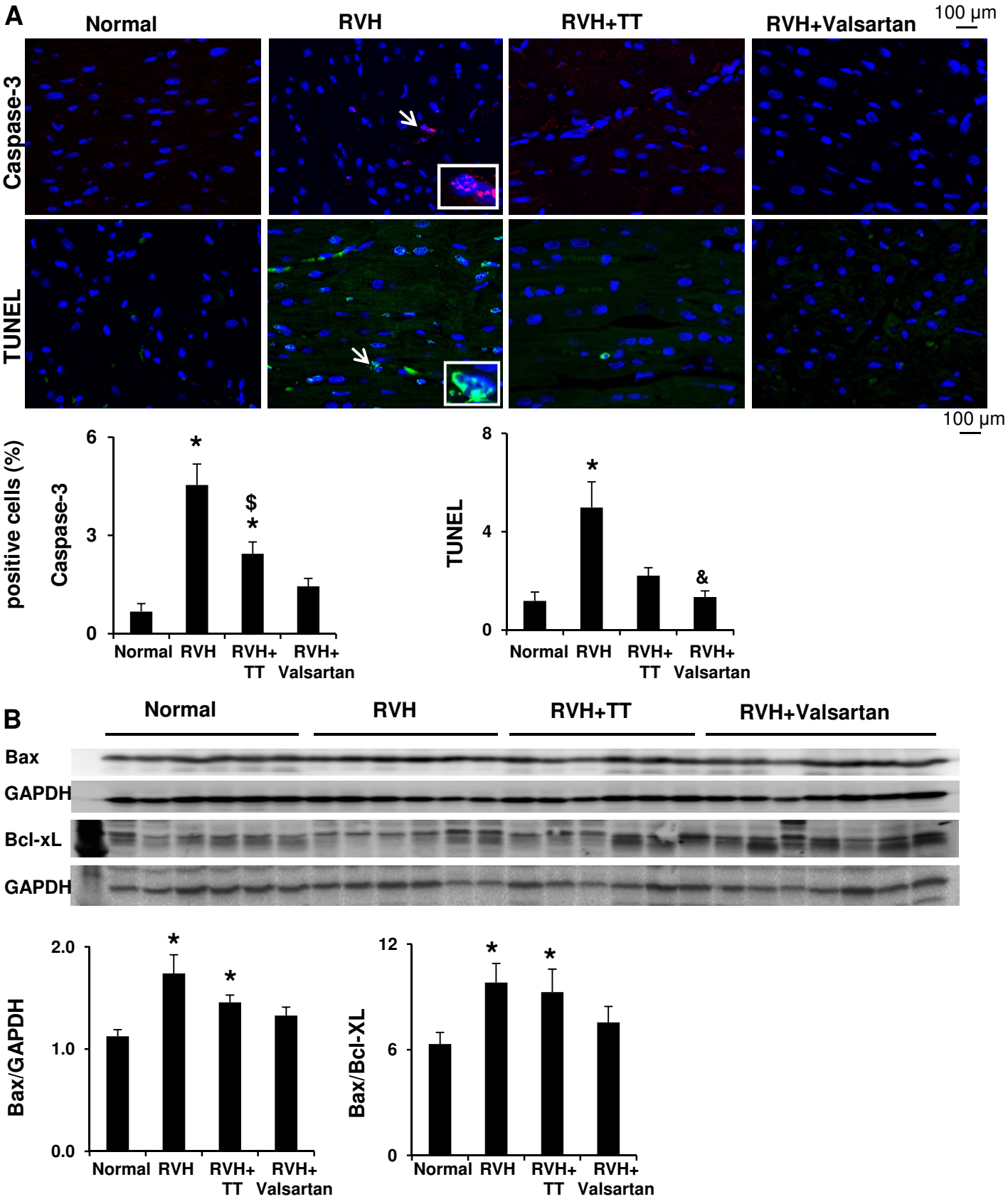

Figure S4. A: Immunofluorescent staining for Caspase-3 (red) and TUNEL (green, blue nuclei), and B: Expression of apoptotic proteins for Bax and Bcl-xL. RVH activated apoptosis. Both regimens alleviated apoptosis, but Valsartan more than TT. *p<0.05 vs. Normal; $p<0.05 vs. RVH; &p<0.05 vs. RVH+TT.

Figure s5

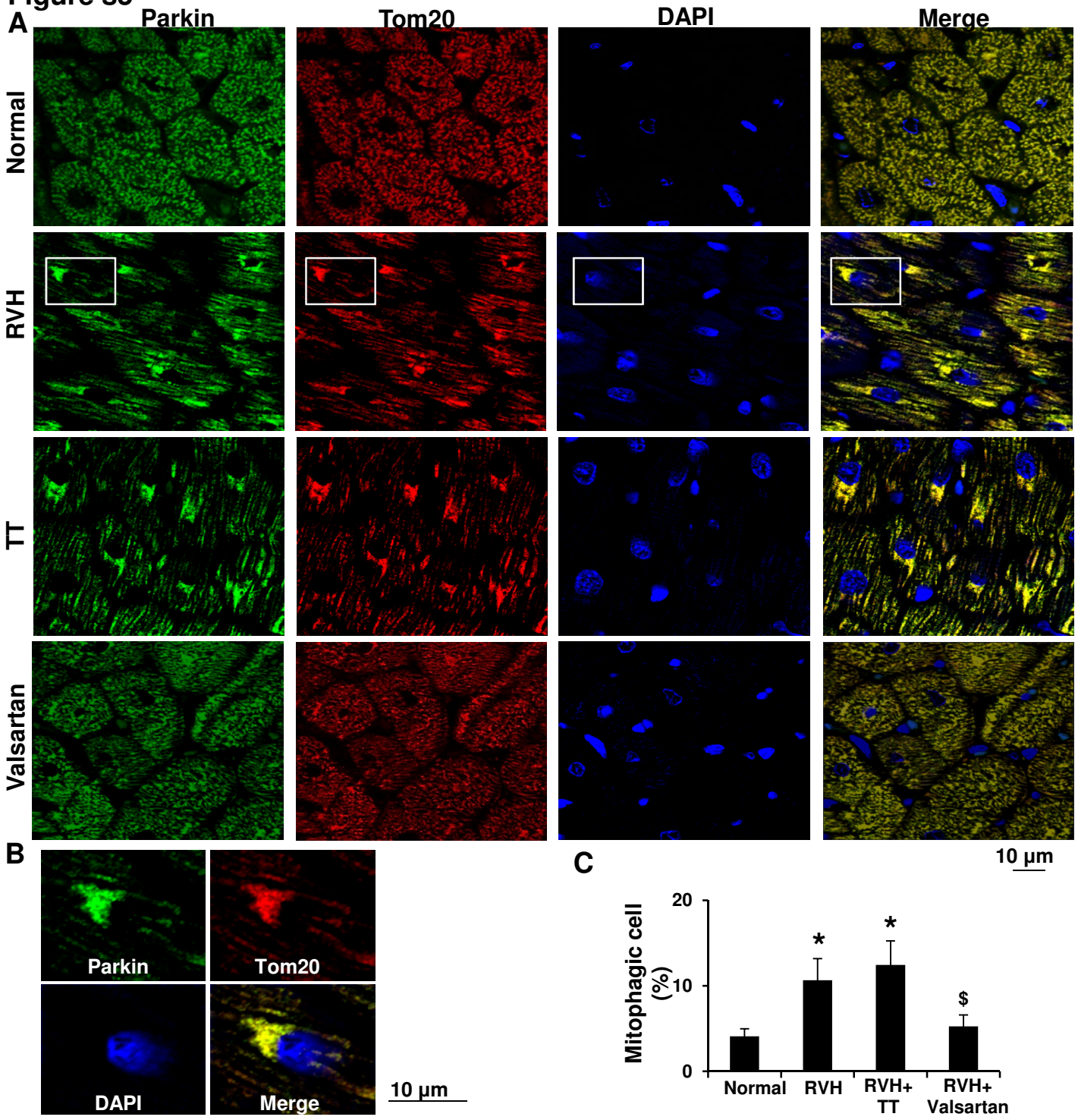

Figure S5. A: Immunofluorescence staining of Parkin (green), the mitochondrial outer membrane marker Tom20 (red), nuclei (blue), and their merged images (40x). Mitophagy induction was indicated by co-localization of Parkin and Tom20. In the top row images, in normal pig cardiomyocytes both Parkin and Tom20 were evenly distributed across the cytosol. Second row images, obtained from an RVH pig, show markedly increased peri-nuclear aggregates (yellow) positively stained for both Parkin and Tom20, indicating translocation of Parkin to damaged mitochondria membrane, and hence mitophagy induction (Inserts shown in panel B). In the third row images, TT did not alter Parkin translocation in RVH. Bottom row images show that Valsartan alleviated the number of mitophagic cells. C: Quantification of mitophagic/Parkin translocation+ cells. *$p<0.05$ vs. Normal; $^{\$}p<0.05$ vs. RVH.

Figure s6

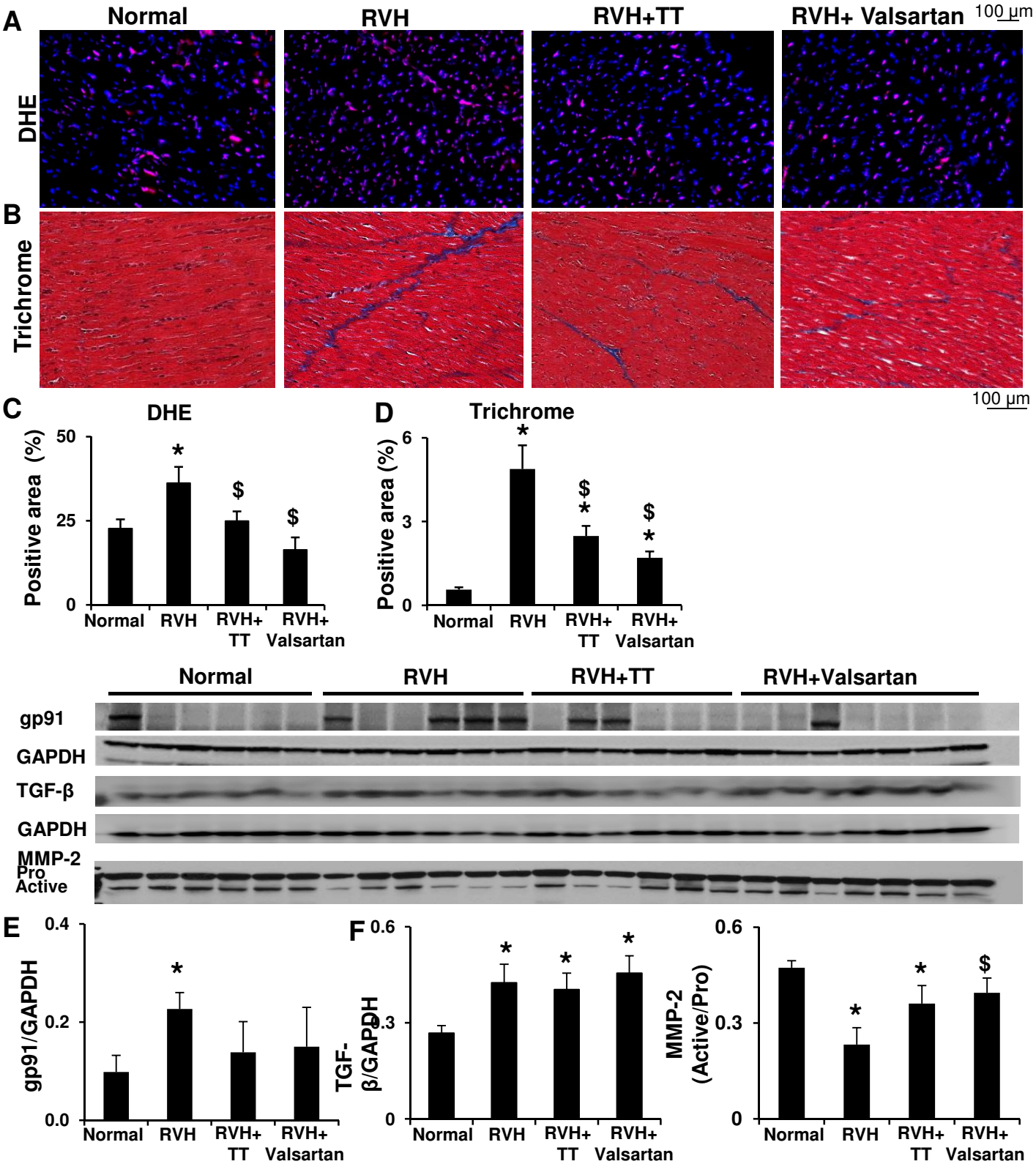

Figure S6. A, C and E: Representative immunofluorescence images (40x) and quantification for dihydroethidium (DHE), and expression of NAD(P)H oxidase gp91. RVH increased oxidative stress, which was alleviated by both regimens. B, D and F: Representative images of myocardial trichrome staining (20x), its quantification, and expression of tissue growth factor (TGF)-β and matrix metalloproteinase (MMP)-2 and activated MMP-2. Myocardial fibrosis in RVH was alleviated by both regimens, but to a slightly greater extent in Valsartan. *$p<0.05$ vs. Normal; $^{\$}p<0.05$ vs. RVH.

Figure S7

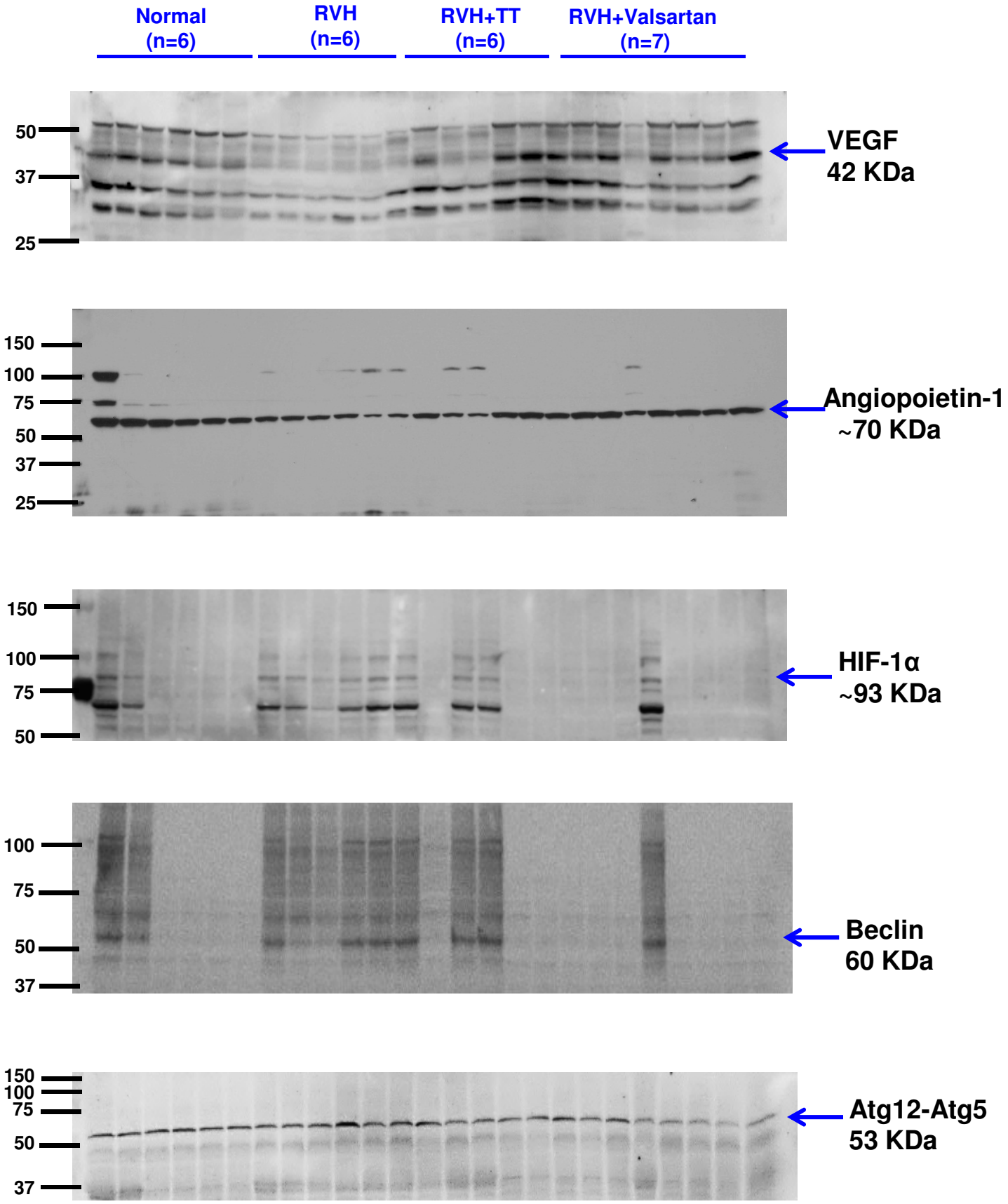
Normal (n=6)
RVH (n=6)
RVH+TT (n=6)
RVH+Valsartan (n=7)
50
37
25
VEGF
42 KDa
150
100
75
50
37
25
Angiopoietin-1
~70 KDa
150
100
75
50
HIF-1α
~93 KDa
100
75
50
37
Beclin
60 KDa
150
100
75
50
37
Atg12-Atg5
53 KDa

Figure S8

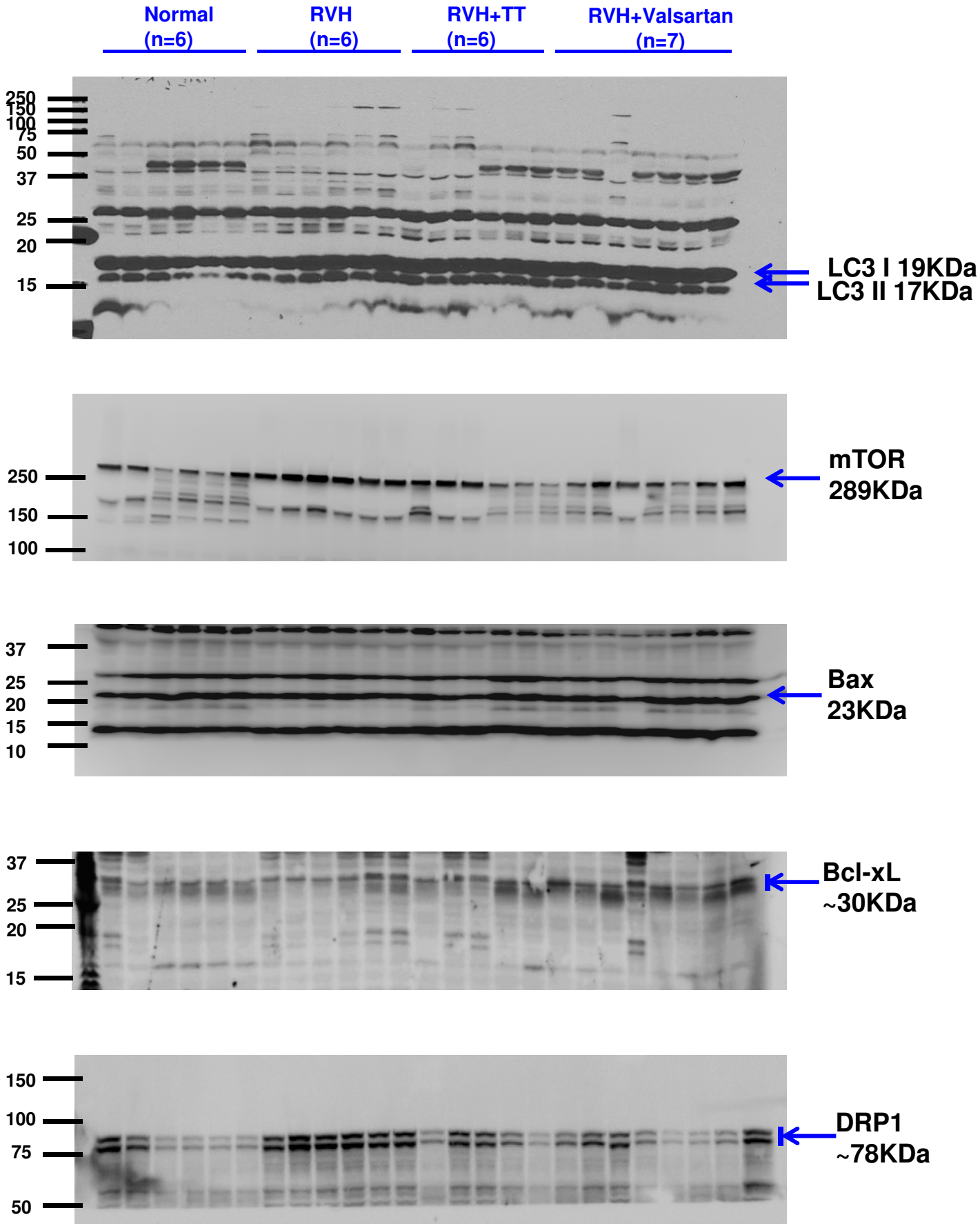
Normal (n=6)
RVH (n=6)
RVH+TT (n=6)
RVH+Valsartan (n=7)
250
150
100
75
50
37
25
20
15
LC3 I 19KDa
LC3 II 17KDa
250
150
100
mTOR
289KDa
37
25
20
15
10
Bax
23KDa
37
25
20
15
Bcl-xL
~30KDa
150
100
75
50
DRP1
~78KDa

Figure S9

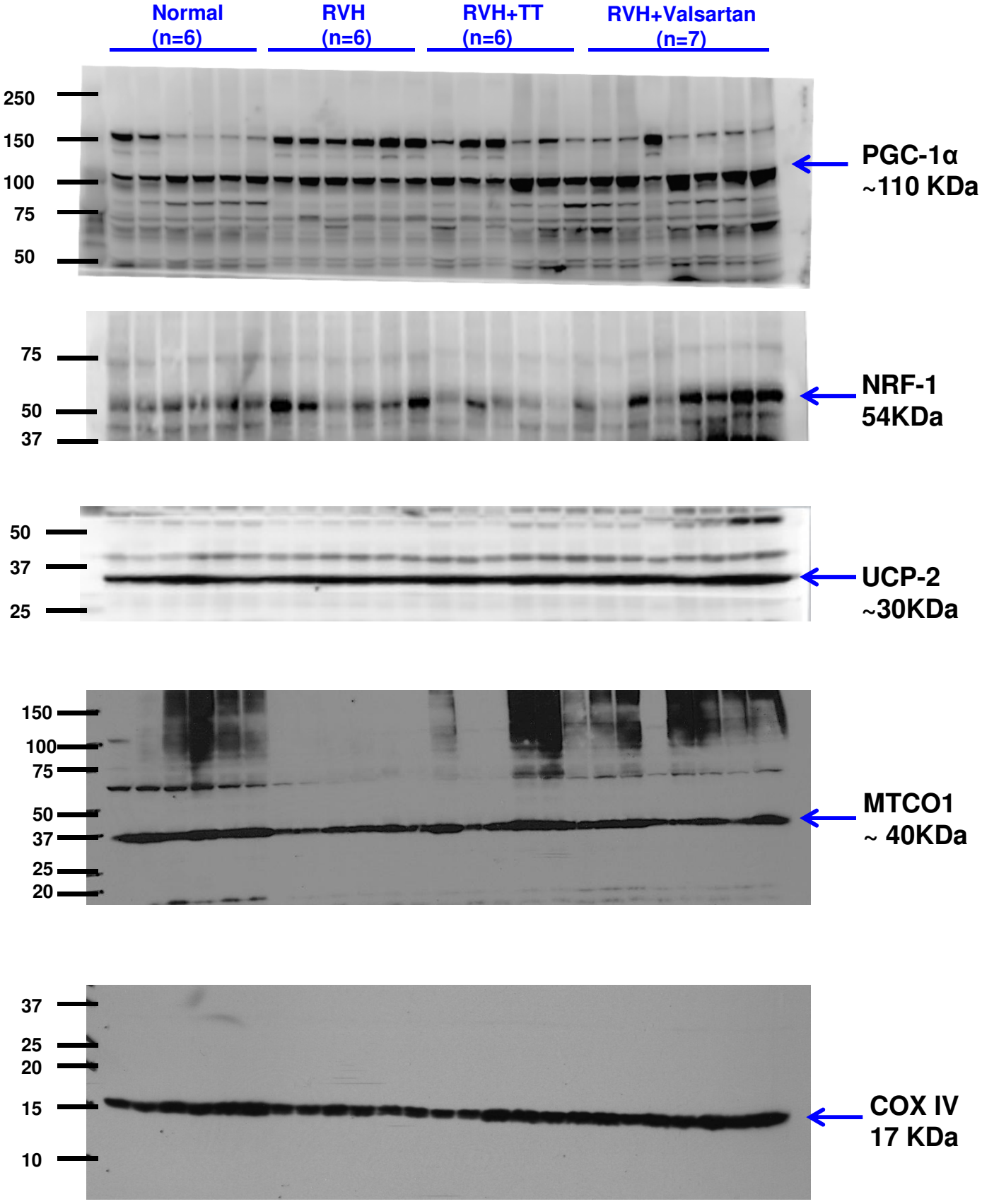
Normal (n=6)
RVH (n=6)
RVH+TT (n=6)
RVH+Valsartan (n=7)
250
150
100
75
50
PGC-1α ~110 KDa
75
50
37
NRF-1 54KDa
50
37
25
UCP-2 ~30KDa
150
100
75
50
37
25
20
MTCO1 ~ 40KDa
37
25
20
15
10
COX IV 17 KDa

Figure S10

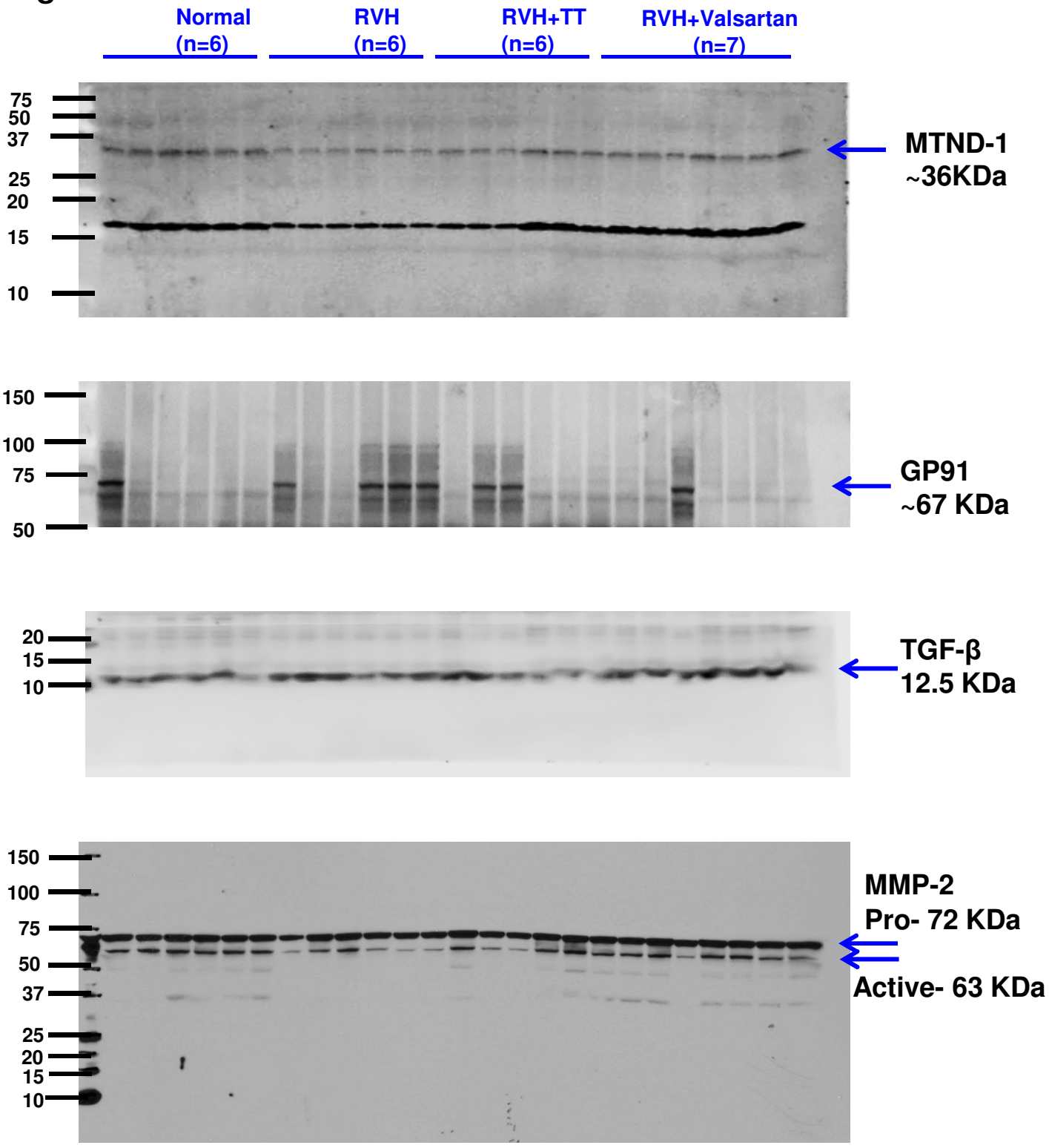

Figure S7-S10. Whole gel images for all proteins examined by western blotting. Images are shown in the order in which the proteins expression is reported in the Results section of the manuscript.